

Physics of \mathcal{PT} -symmetric quantum systems at finite temperatures

Qian Du,^{*} Kui Cao,^{*} and Su-Peng Kou[†]

Center for Advanced Quantum Studies, Department of Physics, Beijing Normal University, Beijing 100875, China

 (Received 22 September 2021; revised 11 July 2022; accepted 19 August 2022; published 7 September 2022)

We study parity-time-symmetric non-Hermitian quantum systems at finite temperature, where the Boltzmann distribution law fails to hold. To characterize their abnormal physical properties, a quantum statistical theory (the so-called quantum Liouvillian statistical theory) is developed, in which the Boltzmann distribution law is replaced by the Liouvillian-Boltzmann distribution law. Using the theory, we derive analytical results of thermodynamic properties for parity-time-symmetric non-Hermitian quantum systems and find that a “continuous” thermodynamic phase transition occurs at the exceptional point, where a zero-temperature anomaly exists.

DOI: [10.1103/PhysRevA.106.032206](https://doi.org/10.1103/PhysRevA.106.032206)

I. INTRODUCTION

In statistical mechanics, the *Boltzmann distribution (BZ) law* plays a central role and governs the equilibrium distribution of different equilibrium states at a particular temperature. According to this law, a system will be in a certain state as a function of its energy E_n and the temperature T . As a result, the weights of different (quantum) states obey the BZ law, i.e., $P_n \sim e^{-E_n/k_B T}$. This universal distribution law was derived by Boltzmann through an axiomatic method, which involves finding the most likely macrostates for a given total energy under the assumption that all possible microstates are equally likely to occur. Using the BZ law, one can recognize properties of macroscopic quantities of different physical systems at finite temperature (finite-T).

The non-Hermitian (NH) problem in controllable open quantum systems has recently emerged as one of the frontiers of physics. A parity-time (\mathcal{PT})-symmetric NH quantum model was proposed by Bender and Boettcher in 1998, where \mathcal{PT} -symmetric spontaneous symmetry breaking (\mathcal{PT} -SSB) occurs at a critical point [the so-called “exceptional point”(EP)] [1–3]. \mathcal{PT} -symmetric systems have attracted considerable attention in different fields [4–8] and various approaches were proposed for realizing \mathcal{PT} -symmetric NH models [9–35]. However, the properties of a \mathcal{PT} -symmetric NH quantum system at finite-T (the so-called *thermal \mathcal{PT} system*) were inadequately reported and nothing is known about their thermodynamic behaviors. Hence, immediate questions appear, such as: *Do the thermal \mathcal{PT} systems still obey the BZ law? If not, what distribution law do they obey? Are there new physical phenomena compared with their Hermitian counterparts for thermal \mathcal{PT} systems?*

In this paper, by considering a typical thermal \mathcal{PT} system as an example, we study this issue and derive reliable results by solving the quantum master equation. According to them, a surprising discovery is that the BZ law is no longer applica-

ble in such systems. As a result, a theory beyond the usual quantum statistical one, the quantum Liouvillian statistical theory, is developed to completely understand these abnormal physical properties of NH systems at finite-T. In particular, there exists the nonthermalization in high temperature. Using the theory, we derive analytical results of thermodynamic properties for thermal \mathcal{PT} systems and find that a “continuous” thermodynamic phase transition occurs at the EP, where a zero-temperature anomaly exists.

The outline of this paper is as follows. In Sec. II, based on a simple Hermitian two-level system, we review quantum statistical theory for Hermitian quantum systems at finite-T. In this section, we show the usual BZ law at the thermodynamic equilibrium. In Sec. III, we point out that there are two choices about the distribution law of NH systems at finite-T. In Sec. IV, to find the correct answer to the two-choice problem, we do a simulation on a typical thermal \mathcal{PT} system based on the quantum master equation. Then, we compare the results with those from the two choices and then find the correct answer. In Sec. V, based on the correct answer, we develop the quantum Liouvillian statistical theory for an arbitrary NH system with finite-T. In Sec. VI, we study the thermodynamic properties of the thermal \mathcal{PT} system and find a “continuous” thermodynamic phase transition at the EP. In Sec. VII, we draw the conclusion.

II. BOLTZMANN DISTRIBUTION LAW IN THE HERMITIAN SYSTEMS

It is well known that in quantum statistical mechanics the canonical ensemble at the thermodynamic equilibrium satisfies the BZ law. For example, we consider a simple Hermitian two-level system

$$\hat{H} = h\sigma_x, \quad (1)$$

where h is a real number. Its density matrix at the thermodynamic equilibrium is

$$\rho = e^{-\beta_r \hat{H}}, \quad (2)$$

^{*}These authors contributed equally to this work.

[†]Corresponding author: spkou@bnu.edu.cn

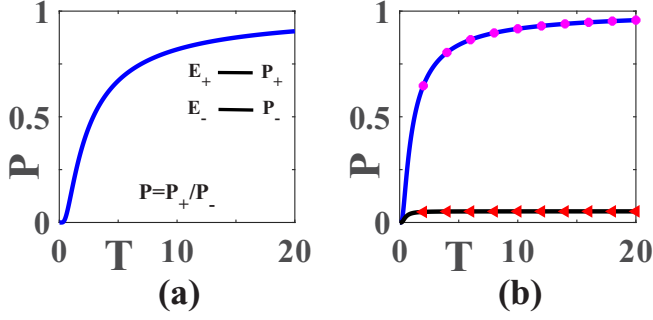


FIG. 1. (a) The relative weight distribution $P = P_+/P_-$ of the simple Hermitian two-level system from Boltzmann distribution (BZ) law. (b) The relative weight distribution P of the thermal \mathcal{PT} system from BZ law $P = P^{BZ}/P^{BZ}$ (blue curve), choice I $P = P^I_+/P^I_-$ (magenta dots), choice II $P = P^{II}_+/P^{II}_-$ (black curve), and Gorini-Kossakowski-Sudarshan-Lindblad equation $P = P^S_+/P^S_-$ (red triangles), where $\gamma = 0.9$.

where $\beta_T = \frac{1}{k_B T}$ is the inverse temperature. The weights of different quantum states obey the BZ law

$$P_n = \frac{1}{Z} \text{eig}_n(\rho) = \frac{1}{Z} \langle n | \rho | n \rangle = \frac{1}{Z} e^{-\beta_T E_n}, \quad (3)$$

where $\text{eig}_n(\rho)$ denotes the eigenvalue of the density matrix ρ , $|n\rangle$ is the eigenstate of ρ ($n = \pm$), $E_n = \pm h$ is the eigenvalue of \hat{H} , and

$$Z = \text{Tr}(\rho) = \sum_{n=\pm} \langle n | e^{-\beta_T \hat{H}} | n \rangle \quad (4)$$

is the partition function. The relative weight distribution

$$P = \frac{P_+}{P_-} \quad (5)$$

is shown in Fig. 1(a). In the paper, we set $h = 1$ and $k_B = 1$. From Fig. 1(a), when the temperature T turns to infinity, P becomes 1. As a result, at very high temperature, all microscopic quantum states have the same weight and the system is completely thermalized.

III. DISTRIBUTION LAW IN THE NON-HERMITIAN SYSTEMS: A TWO-CHOICE PROBLEM

To learn the distribution law in NH quantum systems at finite- T , we first study a \mathcal{PT} system with real energy levels, of which the Hamiltonian is

$$\hat{H}_{\text{NH}} = h\sigma_x + i\gamma\sigma_y, \quad |\gamma| < |h|. \quad (6)$$

By doing a similarity transformation (ST) $\hat{S} = e^{\beta_{\text{NH}} \hat{H}'}$, \hat{H}_{NH} can be transformed into a Hermitian one, i.e.,

$$\hat{H}_0 = \hat{S}^{-1} \hat{H}_{\text{NH}} \hat{S} = \sqrt{h^2 - \gamma^2} \sigma_x. \quad (7)$$

Here, $\beta_{\text{NH}} = \frac{1}{2} \ln \frac{h+\gamma}{h-\gamma}$ characterizes the strength of the NH terms and the Hermitian operator $\hat{H}' = \frac{1}{2} \sigma_z$ determines the form of the NH terms. Under the NH ST \hat{S} , its energy level

$$E_n = \pm \sqrt{h^2 - \gamma^2} \quad (8)$$

is the same as those of a Hermitian system \hat{H}_0 . Its left or right eigenstates $|\Psi_{\pm}^{L/R}\rangle$ under biorthogonal basis can be expressed

by

$$\begin{aligned} \langle \Psi_{\pm}^L | &= \langle \Psi_{0,\pm} | \hat{S}^{-1} = \langle \Psi_{0,\pm} | e^{-\beta_{\text{NH}} \hat{H}'}, \\ |\Psi_{\pm}^R\rangle &= \hat{S} |\Psi_{0,\pm}\rangle = e^{\beta_{\text{NH}} \hat{H}'} |\Psi_{0,\pm}\rangle \end{aligned} \quad (9)$$

with $\langle \Psi_n^L | \Psi_m^R \rangle = \delta_{nm}$ and $\sum_{n=\pm} |\Psi_n^R\rangle \langle \Psi_n^L| = \hat{I}$, where $|\Psi_{0,\pm}\rangle$ are the normalized eigenstates of \hat{H}_0 and \hat{I} is the unit operator.

Based on the characteristics of the biorthogonal basis of NH systems, there are *two* choices for the expression of the density matrix of NH systems at finite- T . Choice I is [36–39]

$$\rho^I = \sum_{n=\pm} |\Psi_n^R\rangle e^{-\beta_T E_n} \langle \Psi_n^L| = \hat{S} (e^{-\beta_T \hat{H}_0}) \hat{S}^{-1}. \quad (10)$$

In addition, we give choice II

$$\rho^{II} = \sum_{n=\pm} |\Psi_n^R\rangle e^{-\beta_T E_n} \langle \Psi_n^R| = \hat{S} (e^{-\beta_T \hat{H}_0}) \hat{S}^\dagger. \quad (11)$$

After considering the fact of $|\Psi_{\pm}^R\rangle \neq |\Psi_{\pm}^L\rangle$ and the definition of ρ^I , we find that ρ^I is NH, i.e., $(\rho^I)^\dagger \neq \rho^I$. We notice that for the case of choice I, the usual BZ law does not change. Now, the weight of a quantum state in choice I is

$$\begin{aligned} P_n^I &= \frac{1}{\text{Tr}(\rho^I)} \text{eig}_n(\rho^I) = \frac{1}{\text{Tr}(\rho^I)} \langle n_I^L | \rho^I | n_I^R \rangle \\ &\equiv P_n^{\text{BZ}} = \frac{1}{\text{Tr}(\rho^{\text{BZ}})} e^{-\beta_T E_n}, \end{aligned} \quad (12)$$

where $|n_I^{L/R}\rangle$ are the left or right eigenstates of ρ^I and $\rho^{\text{BZ}} = e^{-\beta_T \hat{H}_{\text{NH}}}$ is the density matrix from the BZ law. This equivalent relation can be obtained from the fact of

$$\rho^I = \hat{S} (e^{-\beta_T \hat{H}_0}) \hat{S}^{-1} = e^{-\beta_T \hat{H}_{\text{NH}}} = \rho^{\text{BZ}}. \quad (13)$$

On the other hand, the weight of a quantum state in choice II is

$$P_n^{II} = \frac{1}{\text{Tr}(\rho^{II})} \text{eig}_n(\rho^{II}) = \frac{1}{\text{Tr}(\rho^{II})} \langle n_{II} | \rho^{II} | n_{II} \rangle, \quad (14)$$

where $|n_{II}\rangle$ is the eigenstate of ρ^{II} . Here, we emphasize that ρ^{II} is a Hermitian operator, i.e., $(\rho^{II})^\dagger = \rho^{II}$.

To make it clear, we plot the relative weight distributions from different starting points, choice I (or the case of BZ law) and choice II in Fig. 1(b). Obviously, the results from choice I are quite different from those from choice II. *Which one is right that could characterize correctly the experiments of NH systems at finite- T ?*

IV. FINDING THE CORRECT ANSWER BY SIMULATING THE THERMAL PARITY-TIME SYSTEM

The density matrix ρ^I in choice I is always NH, $(\rho^I)^\dagger \neq \rho^I$; while the density matrix ρ^{II} in choice II is Hermitian, $(\rho^{II})^\dagger = \rho^{II}$. Therefore, we may guess choice II with the density matrix as ρ^{II} is correct. To check the conclusion, we do a simulation of the thermal \mathcal{PT} system. First, to design a thermal \mathcal{PT} system, we control an open quantum system coupling to two separate environments and obtain an *open NH quantum system*. Then, we solve the quantum master equation of the open NH quantum system. After obtaining its density matrix ρ^S , we compare the results with those from choice I or choice II and finally find the correct answer.

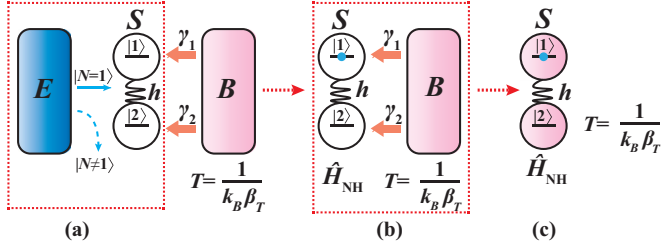


FIG. 2. Illustration of a thermal \mathcal{PT} system that comes from the controllable open quantum system S coupling to two separate environments B and E . S denotes a tight-binding model of two lattice sites 1,2 with a single fermion. There is only one fermion at lattice 1 or lattice 2, so S is a two-level system. B denotes an environment with temperature $T = \frac{1}{k_B \beta_T}$, which could thermalize S to its temperature T (we call it *thermal environment*). E denotes an environment that could lead to a relevant non-Hermitian (NH) term for S under postselection with the particle number of S fixed at $N = 1$ (we call it *NH environment*). (a) The total system consists of S , B , and E . (b) The combined subsystem $S + B$ after tracing out E and postselection measurements. (c) The thermal \mathcal{PT} system after tracing out B .

A. Experimental design of the thermal parity-time system

To design a thermal \mathcal{PT} system, we consider a controllable open quantum system S coupling to two separate environments B and E . See the illustration in Fig. 2(a). The Hamiltonian of the total system is given by

$$\hat{H} = \hat{H}_S \otimes \hat{I}_E \otimes \hat{I}_B + \hat{I}_S \otimes \hat{H}_E \otimes \hat{I}_B + \hat{I}_S \otimes \hat{I}_E \otimes \hat{H}_B + \hat{H}_{ES} \otimes \hat{I}_B + \hat{I}_E \otimes \hat{H}_{BS}, \quad (15)$$

where $\hat{H}_S = h(c_1^\dagger c_2 + c_2^\dagger c_1)$, \hat{H}_E , and \hat{H}_B are the Hamiltonians of S , E , and B , respectively. $\hat{I}_{S,E,B}$ are the unit operators of S , E , and B , respectively. $c_{1,2}^\dagger, c_{1,2}$ are the creation (annihilation) operators of the fermion in S . $\hat{H}_{ES} = \lambda[a^\dagger(c_1 - ic_2) + \text{H.c.}]$ stands for the coupling between S and E that leads to a Lindblad operator $\hat{L}_{ES} = \sqrt{2\gamma}(c_1 + ic_2) \otimes \hat{I}_B$, where γ is the coupling strength and $a^\dagger(a)$ is the creation (annihilation) operator in E . $\hat{H}_{BS} = \sum_{i=1,2} \gamma_i c_i^\dagger c_i \otimes \hat{B}_i$ describes the coupling between S and B , where $\hat{B}_{1,2}$ are operators of B and $\gamma_{1,2}$ are the coupling strength. Here, we assume that $\gamma_1, \gamma_2 \ll \gamma, h$. There is *no direct coupling* between the two environments B and E .

We point out that the thermal \mathcal{PT} system can be implemented experimentally based on ultracold atoms in optical lattices with the engineered dissipation proposed by the authors of Ref. [40] together with an extra thermal cavity. Engineering \hat{L}_{ES} can obtain the effective NH Hamiltonian under postselection, which can be realized using a nonlocal Rabi coupling to some auxiliary degrees of freedom with rapid local loss. After adiabatically eliminating the fast decay modes, effective dynamics with target degrees of freedom alone are obtained. The thermal environment can be provided by a cavity with finite- T .

For the open quantum system S under the Markovian approximation, its nonunitary dynamics is in general expressed by the quantum master equation in the Gorini-Kossakowski-

Sudarshan-Lindblad (GKSL) form [41–43]

$$\frac{d\rho^S(t)}{dt} \equiv \mathcal{L}\rho^S(t), \quad (16)$$

where \mathcal{L} is a Liouville superoperator acting on the (reduced) density matrix ρ^S of the subsystem S .

For the total system $S + B + E$, we trace out the NH environment E from it and consider its effect on the combined subsystem $S + B$. We make the postselection measurement for the number of particles $\hat{N} = (c_1^\dagger c_1 + c_2^\dagger c_2) \otimes \hat{I}_B$ in S , so that it is always $N = 1$ [44]. After the postselection measurements, the quantum jumping term will be projected out [45]. Then ρ^{S+B} becomes

$$\frac{d\rho^{S+B}}{dt} = -i(\hat{H}_{S+B,\text{eff}}\rho^{S+B} - \rho^{S+B}\hat{H}_{S+B,\text{eff}}^\dagger), \quad (17)$$

where

$$\hat{H}_{S+B,\text{eff}} = \hat{H}_{\text{NH}} \otimes \hat{I}_B + \hat{I}_S \otimes \hat{H}_B + \hat{H}_{BS} \quad (18)$$

is the effective Hamiltonian of the combined subsystem $S + B$, and

$$\hat{H}_{\text{NH}} = (h + \gamma)c_1^\dagger c_2 + (h - \gamma)c_2^\dagger c_1 - i\gamma \quad (19)$$

can effectively describe S in Fig. 2(b). Here, the term $-i\gamma$ can be ignored due to the postselection measurements [46,47]. We assume that the temperature of a possible thermodynamic equilibrium state of S is the same as that of the thermal environment B . Thus, we gain a thermal \mathcal{PT} system in Fig. 2(c), which can also be expressed effectively as

$$\hat{H}_{\text{NH}} = h\sigma_x + i\gamma\sigma_y \quad (20)$$

on the pseudospin space ($\begin{smallmatrix} \uparrow \\ \downarrow \end{smallmatrix}$) where $|\uparrow\rangle$ and $|\downarrow\rangle$ denote the quantum states of the single fermion on site 1 and site 2, respectively. For \hat{H}_{NH} , at $h = \gamma$, a usual \mathcal{PT} -SSB occurs: for the case of $h > \gamma$, the energy levels $|+\rangle$ and $|-\rangle$ are $E_\pm = \pm\sqrt{h^2 - \gamma^2}$; for the case of $h < \gamma$, the energy levels $|+\rangle$ and $|-\rangle$ are $E_\pm = \pm i\sqrt{\gamma^2 - h^2}$; and for the case of $h = \gamma$, the system is at the EP with state coalescing and energy degeneracy, i.e., $E_\pm = 0$.

B. Quantum master equation in the Gorini-Kossakowski-Sudarshan-Lindblad form of the open non-Hermitian quantum system

In this subsection, we solve the quantum master equation in the GKSL form of the thermal \mathcal{PT} system with \mathcal{PT} symmetry ($h > \gamma$) and calculate the Liouville superoperator \mathcal{L} under the Born-Markov approximation in the interaction picture, which has never been studied before.

We trace over the degrees of freedom of the thermal environment B from Eq. (17), and consider its effect on the NH subsystem S . We assume that S has little influence on B , and average out the high-frequency part of the quantum transition processes by the rotating wave approximation [43]. Eventually, the reduced density matrix $\rho_{In}^S(t)$ of the subsystem

S in the interaction picture is

$$\frac{d}{dt}\rho_{In}^S(t) = \sum_{a,b} \sum_{\omega} [\Gamma_{ab}(\omega)[\hat{A}_b(\omega)\rho_{In}^S(t)\hat{A}_a^\dagger(\omega) - \hat{A}_a(-\omega)\hat{A}_b(\omega)\rho_{In}^S(t)] + \text{H.c.}], \quad (21)$$

where $\Gamma_{ab}(\omega)$ are the one-sided Fourier transforms

$$\Gamma_{ab}(\omega) = \int_0^t ds e^{i\omega s} \langle \hat{B}_a^\dagger(s)\hat{B}_b(0) \rangle \quad (22)$$

$$\mathcal{L} = \begin{pmatrix} -\gamma_0(1 + e^{\omega_0/k_B T}) & 0 & 0 & \gamma_0(1 + e^{\omega_0/k_B T})\frac{h+\gamma}{h-\gamma} \\ -2\gamma_0(e^{\omega_0/k_B T} - 1)\sqrt{\frac{h-\gamma}{h+\gamma}} & -3\gamma_0(1 + e^{\omega_0/k_B T}) & -\gamma_0(1 + e^{\omega_0/k_B T}) & -2\gamma_0(e^{\omega_0/k_B T} - 1)\sqrt{\frac{h+\gamma}{h-\gamma}} \\ -2\gamma_0(e^{\omega_0/k_B T} - 1)\sqrt{\frac{h-\gamma}{h+\gamma}} & -\gamma_0(1 + e^{\omega_0/k_B T}) & -3\gamma_0(1 + e^{\omega_0/k_B T}) & -2\gamma_0(e^{\omega_0/k_B T} - 1)\sqrt{\frac{h+\gamma}{h-\gamma}} \\ \gamma_0(1 + e^{\omega_0/k_B T})\frac{h-\gamma}{h+\gamma} & 0 & 0 & -\gamma_0(1 + e^{\omega_0/k_B T}) \end{pmatrix} \quad (25)$$

in the region of $h > \gamma$, where

$$\gamma_0 = \frac{1}{16} \{ \gamma_{11}(-\omega_0)\gamma_1^2 + \gamma_{22}(-\omega_0)\gamma_2^2 - [\gamma_{12}(-\omega_0) + \gamma_{21}(-\omega_0)]\gamma_1\gamma_2 \}.$$

See the detailed calculations regarding the quantum master equation in Appendix A.

C. Non-Hermitian thermal state and the correct answer

In Hermitian systems at finite-T, the quantum statistical mechanics is based on the thermal equilibrium state. To reach it, one can prepare a unique final state under time evolution (from an arbitrary initial state). Using similar logic, we introduce a “*non-Hermitian thermal state*” (NHTS), which is the unique final state under time evolution in NH systems at finite-T (from an arbitrary initial state). We find that if the spectrum of Liouville superoperator \mathcal{L} is λ_i , i.e.,

$$\mathcal{L}\rho_i^S = \lambda_i\rho_i^S, \quad (26)$$

then a NHTS described by ρ_{NHTS}^S is the eigenstate of \mathcal{L} corresponding to the eigenvalue with the maximum real part $\lambda_{\text{NHTS}} = \max(\text{Re } \lambda_i)$.

For the case of \mathcal{PT} symmetry ($h > \gamma$), two energy levels of \hat{H}_{NH} are purely real, $E_n = \pm\sqrt{h^2 - \gamma^2}$. The eigenvalues of \mathcal{L} in Eq. (25) are

$$-4\gamma_0(1 + e^{\omega_0/T}), \quad -2\gamma_0(1 + e^{\omega_0/T}), \quad -2\gamma_0(1 + e^{\omega_0/T}), \quad 0.$$

The first three will dissipate and the rest will form a NHTS that is also a steady state. Thus, the density matrix ρ_{NHTS}^S for a NHTS corresponding to the eigenvalue of the Liouville

of the reservoir correlation functions

$$\langle \hat{B}_a^\dagger(s)\hat{B}_b(0) \rangle = \text{Tr}_B(\hat{B}_a^\dagger(t)\hat{B}_b(t-s)\rho_{In}^B) \quad (23)$$

of B with $a, b = 1$ or 2 . $\hat{A}_{a,b}(\omega)$ is a NH operator as

$$\hat{A}_a(\omega) = \sum_{m=\pm} |m\rangle_R \langle m|_L \gamma_a c_a^\dagger c_a |m+\omega\rangle_R \langle m+\omega|_L. \quad (24)$$

$|m\rangle_{R,L}$ are the right or left eigenstates of \hat{H}_{NH} with the eigenvalue E_m , and $|m+\omega\rangle_{R,L}$ are the right or left eigenstates of \hat{H}_{NH} with the eigenvalue $E_{m+\omega}$. They satisfy ${}_L\langle m|m\rangle_R = 1$. In addition, we have $\omega = \pm\omega_0$, 0 with $\omega_0 = |E_+ - E_-| = 2\sqrt{h^2 - \gamma^2}$.

According to $\frac{d\rho_{In}^S(t)}{dt} \equiv \mathcal{L}\rho_{In}^S(t)$, we simplify and obtain

superoperator \mathcal{L} with maximum real part is obtained as

$$\rho_{\text{NHTS}}^S = \frac{h-\gamma}{2h} \begin{pmatrix} \frac{h+\gamma}{h-\gamma} & \sqrt{\frac{h+\gamma}{h-\gamma}} \frac{1-e^{\omega_0\beta T}}{1+e^{\omega_0\beta T}} \\ \sqrt{\frac{h+\gamma}{h-\gamma}} \frac{1-e^{\omega_0\beta T}}{1+e^{\omega_0\beta T}} & 1 \end{pmatrix}. \quad (27)$$

According to the results obtained from the GKSL equation and the definition of the NHTS, we obtain the weight of a quantum state

$$P_n^S = \frac{1}{\text{Tr}(\rho_{\text{NHTS}}^S)} \langle n_S | \rho_{\text{NHTS}}^S | n_S \rangle, \quad (28)$$

where $|n_S\rangle$ is the eigenstate of ρ_{NHTS}^S . The results of the relative weight distribution of the GKSL equation $P = P_+^S/P_-^S$ are plotted in Fig. 1(b). It is obvious that the results from choice I are quite different from numerical results from the GKSL equation; while the results from choice II are the same as those from the GKSL equation. In particular, the consistency between the different results verifies the correctness of the definition of ρ^{II} in choice II rather than ρ^{I} in choice I, i.e.,

$$\rho^{\text{I}} = \rho^{\text{BZ}} \neq \rho_{\text{NHTS}}^S, \quad \rho^{\text{II}} = \rho_{\text{NHTS}}^S \quad (29)$$

or

$$P_n^{\text{I}} = P_n^{\text{BZ}} \neq P_n^S, \quad P_n^{\text{II}} = P_n^S. \quad (30)$$

Consequently, one can safely conclude that the usual BZ law in Hermitian systems does not work any longer in NH systems and there exists a new law that explains these abnormal results for a thermal \mathcal{PT} system. In fact, NHTSs come from NH systems rather than from free ones. To realize a NH system, we may control the open thermal \mathcal{PT} system by performing a postselection and projecting out the quantum jumping term. As a result, the equal probability of different microscopic states is broken down and a new distribution law appears.

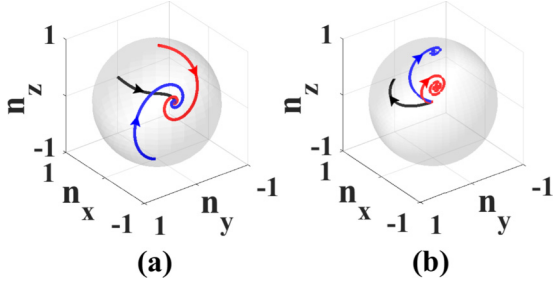


FIG. 3. The expected values $n_i = \langle \sigma_i \rangle$ ($i = x, y, z$) of the spin operators for the thermal \mathcal{PT} system. (a) Time evolution of $n_i = \langle \sigma_i \rangle$ for fixed γ ($\gamma = 0.2$) from the different initial states: the red curve corresponding to $\rho^S(t=0) = (1, 0, 0, 0)$, the blue curve corresponding to $\rho^S(t=0) = (0, 0, 0, 1)$, the black curve corresponding to $\rho^S(t=0) = (\frac{1}{2}, \frac{1}{2}, \frac{1}{2}, \frac{1}{2})$, where $\gamma_0 = 0.05$ and $T = 1$. (b) Time evolution of $n_i = \langle \sigma_i \rangle$ for different γ from the same fully thermalized initial state $\rho^S(t=0) = (\frac{1}{2}, 0, 0, \frac{1}{2})$: the red curve corresponding to $\gamma = 0.3$, the blue curve corresponding to $\gamma = 0.9$, the black curve corresponding to $\gamma = 1.5$, where $\gamma_0 = 0.05$ and $T = 10$. The arrows denote the direction of time evolution.

In addition, we also study the possible NHTS ρ_{NHTS}^S in the phase with \mathcal{PT} -symmetric breaking ($h < \gamma$). Under the condition $\gamma_1, \gamma_2 \ll \gamma, h$, the dissipation term in the Liouville superoperator only has little effect, i.e.,

$$\mathcal{L}\rho^S \approx -i(\hat{H}_{\text{NH}}\rho^S - \rho^S\hat{H}_{\text{NH}}^\dagger). \quad (31)$$

The eigenvalues of the superoperator \mathcal{L} are approximately obtained as

$$-2\sqrt{\gamma^2 - h^2}, \quad 0, \quad 0, \quad 2\sqrt{\gamma^2 - h^2}.$$

The eigenstate with the maximum real part $2\sqrt{\gamma^2 - h^2}$ corresponds to a NHTS with

$$\rho_{\text{NHTS}}^S = |\Psi_+^R\rangle\langle\Psi_+^R|, \quad (32)$$

i.e., the system reaches a pure state $|\Psi_+^R\rangle$ which corresponds to the eigenvalue with the largest imaginary part $+i\sqrt{\gamma^2 - h^2}$ under a long time evolution $t \rightarrow \infty$. This can be understood as the fact that the state $|\Psi_-^R\rangle$ decays more faster than the state $|\Psi_+^R\rangle$. Eventually, there is only one eigenstate $|\Psi_+^R\rangle$ with the largest imaginary part of the eigenvalue $+i\sqrt{\gamma^2 - h^2}$ left in the system.

According to the discussions about the case of \mathcal{PT} symmetry and \mathcal{PT} -symmetric breaking, we investigate the properties of NHTSs in the thermal \mathcal{PT} system. These results of expected values of σ_i ($i = x, y, z$), i.e.,

$$n_i = \langle \sigma_i \rangle = \frac{1}{Z^S} \text{Tr}(\sigma_i \cdot \rho^S), \quad (33)$$

are represented by points on the Bloch sphere in Fig. 3. Figure 3(a) indicates the existence of a *unique* NHTS ρ_{NHTS}^S : for \hat{H}_{NH} with fixed γ ($\gamma = 0.2$), taking the limit $t \rightarrow \infty$, different initial states will eventually evolve into the same final state $\rho^S(t \rightarrow \infty)$. This means $\rho^S(t \rightarrow \infty)$ is just the NHTS ρ_{NHTS}^S ; Fig. 3(b) indicates the *abnormality* of the NHTS ρ_{NHTS}^S : for \hat{H}_{NH} with different γ from the same initial state, for example, a fully thermalized state described by $\rho^S(t=0) = \frac{1}{2}\hat{I}_{2 \times 2}$, the system will eventually evolve into different NHTSs $\rho_{\text{NHTS}}^S(\gamma)$.

V. QUANTUM LIOUVILLIAN STATISTICAL THEORY FOR AN ARBITRARY NH SYSTEM WITH FINITE-T

To better describe the NH system at finite-T, we develop the quantum Liouvillian statistical theory, in which an alternative type of distribution, the *Liouvillian-Boltzmann distribution* (LBZ), governs the distribution of NHTSs.

We assume that the Hamiltonian of the NH system is \hat{H}_{NH} with $\hat{H}_{\text{NH}} \neq \hat{H}_{\text{NH}}^\dagger$. For the NH Hamiltonian \hat{H}_{NH} (or $\hat{H}_{\text{NH}}^\dagger$), we define the left or right eigenstates $|\Psi^{L/R}\rangle$ as

$$\hat{H}_{\text{NH}}^\dagger |\Psi_n^L\rangle = \mathcal{E}_n^* |\Psi_n^L\rangle, \quad \hat{H}_{\text{NH}} |\Psi_n^R\rangle = \mathcal{E}_n |\Psi_n^R\rangle, \quad (34)$$

where $\mathcal{E}_n = \text{Re } \mathcal{E}_n + i \text{Im } \mathcal{E}_n$ and $\mathcal{E}_n^* = \text{Re } \mathcal{E}_n^* - i \text{Im } \mathcal{E}_n^*$ are the corresponding eigenvalues.

For all NH systems, there are a total of three different cases: Case I from the NH systems with real eigenvalues, i.e., $\text{Im } \mathcal{E}_n \equiv 0$; Case II from NH systems with complex eigenvalues and the quantum state with the maximum imaginary part of all eigenvalues is nondegenerate; and Case III from NH systems with complex eigenvalues and quantum states with the maximum imaginary part of all eigenvalues are degenerate. In the following part, we discuss the quantum Liouvillian statistical theory case by case.

A. Case I: Real eigenvalues

We discuss the case of the NH Hamiltonian \hat{H}_{NH} with all real eigenvalues, i.e., $\text{Im } \mathcal{E}_n \equiv 0$. As a result, this is a quasi-Hermitian system. Under the ST \hat{S} , the energy levels \mathcal{E}_n of \hat{H}_{NH} (or $\hat{H}_{\text{NH}}^\dagger$) are all real and the same as those of the Hermitian model \hat{H}_0 , i.e.,

$$\hat{H}_{\text{NH}} = \hat{S}\hat{H}_0\hat{S}^{-1}, \quad (35)$$

with $\hat{H}_0 = \hat{H}_0^\dagger$. The corresponding eigenstates of \hat{H}_{NH} and $\hat{H}_{\text{NH}}^\dagger$ become

$$|\Psi_n^R\rangle = \hat{S}|\Psi_{0,n}\rangle, \quad \langle\Psi_n^L| = \langle\Psi_{0,n}|\hat{S}^{-1}, \quad (36)$$

under the biorthogonal set $\langle\Psi_n^L|\Psi_m^R\rangle = \delta_{nm}$. Here $|\Psi_{0,n}\rangle$ denotes the normalized eigenstate of \hat{H}_0 . In addition, we point out that a quasi-Hermitian model \hat{H}_{NH} with real eigenvalues obeys

$$\hat{\eta}\hat{H}_{\text{NH}}\hat{\eta}^{-1} = \hat{H}_{\text{NH}}^\dagger, \quad (37)$$

which shows NH similarity, where $\hat{\eta} = \sum_n |\Psi_n^L\rangle\langle\Psi_n^L|$. As a result, for \hat{H}_{NH} , the ST is obtained as

$$\hat{S} = \hat{\eta}^{-\frac{1}{2}} = \left(\sum_n |\Psi_n^R\rangle\langle\Psi_n^R| \right)^{1/2}. \quad (38)$$

Now, the density matrix in the NHTS at temperature $T = \frac{1}{k_B\beta_T}$ is given as

$$\rho_{\text{NHTS}}^S = \sum_n |\Psi_n^R\rangle e^{-\beta_T \mathcal{E}_n} \langle\Psi_n^R| = \hat{S}\rho_0\hat{S}^\dagger, \quad (39)$$

where $\rho_0 = e^{-\beta_T \hat{H}_0}$ is the density matrix for the Hermitian model \hat{H}_0 at the thermodynamic equilibrium.

To simplify the Liouvillian physics for NHTSs, we introduce an effective Hamiltonian \hat{H}_L as $e^{-\beta_T \hat{H}_L} = \hat{S}(e^{-\beta_T \hat{H}_0})\hat{S}^\dagger$

or

$$\hat{\mathcal{H}}_L = -\frac{1}{\beta_T} \ln[\hat{S}(e^{-\beta_T \hat{\mathcal{H}}_0})\hat{S}^\dagger]. \quad (40)$$

In this paper, we call the temperature-dependent Hamiltonian $\hat{\mathcal{H}}_L$ the *Liouvillian Hamiltonian* (LH). Its corresponding eigenvalue \mathcal{E}_n^L and eigenstate are called the *Liouvillian energy level* and *Liouvillian state*, respectively. According to $\hat{\mathcal{H}}_L = \hat{\mathcal{H}}_L^\dagger$, \mathcal{E}_n^L must be real.

For NHTSs in this NH system, although the energy levels do not change under STs, the weights and the eigenstates are deformed. Consequently, the usual BZ law $P_n = \frac{1}{Z} e^{-\beta_T \mathcal{E}_n}$ is replaced by the LBZ law [48,49], i.e.,

$$P_n = \frac{1}{Z} e^{-\beta_T \mathcal{E}_n} \rightarrow P_n = \frac{1}{Z_{\text{NHTS}}^S} e^{-\beta_T \mathcal{E}_n^L}, \quad (41)$$

where \mathcal{E}_n^L is a Liouvillian energy level rather than the energy level \mathcal{E}_n and $Z_{\text{NHTS}}^S = \text{Tr}(\rho_{\text{NHTS}}^S)$ is the partition function for the NHTS. To distinguish the phenomenon of weights in the thermal \mathcal{PT} system from those in Hermitian thermal systems, we call the corresponding weight $P_n = \frac{1}{Z_{\text{NHTS}}^S} e^{-\beta_T \mathcal{E}_n^L}$ the *Liouvillian weight*.

In particular, when the temperature is high, $\beta_T \rightarrow 0$, the density matrix ρ_{NHTS}^S for a NH system with real spectra is reduced to

$$\rho_{\text{NHTS}}^S \sim \hat{S} \hat{S}^\dagger = e^{2\beta_{\text{NH}} \hat{H}'},$$

and the Liouvillian weight turns into

$$P_n = \frac{1}{Z_{\text{NHTS}}^S} e^{-\beta_{\text{NH}}(-2E'_n)},$$

where E'_n is the “energy level” of \hat{H}' . We call the abnormality of the NHTS *nonthermalization in high temperature*.

B. Case II: Complex eigenvalues and the nondegenerate quantum state with the maximum imaginary part of all eigenvalues

The NH Hamiltonian $\hat{\mathcal{H}}_{\text{NH}}$ has complex eigenvalues, i.e., $\text{Im } \mathcal{E}_n \neq 0$ ($n = 1, 2, \dots, N$), and $|\Psi_0^R\rangle$ is the nondegenerate quantum state with maximum imaginary part of all eigenvalues, i.e., $\text{Im } \mathcal{E}_0 > \text{Im } \mathcal{E}_{n \neq 0}$. Now, the density matrix in the NHTS is obtained as

$$\rho_{\text{NHTS}}^S = |\Psi_0^R\rangle\langle\Psi_0^R|. \quad (42)$$

Let us give a brief discussion on this result. In the limit of $t \rightarrow \infty$, the system reaches a NHTS and there is only the eigenstate $|\Psi_0^R\rangle$ corresponding to the eigenvalue with maximum imaginary part $\max(\text{Im } \mathcal{E}_n) = \text{Im } \mathcal{E}_0$ left in the system because other states will decay much faster than this state, i.e.,

$$\begin{aligned} |\Psi^R\rangle &= \sum_{n=1}^N \alpha_n |\Psi_n^R\rangle e^{-i\mathcal{E}_n t} \\ &= \sum_{n=1}^N \alpha_n |\Psi_n^R\rangle e^{t \text{Im } \mathcal{E}_n} e^{-it \text{Re } \mathcal{E}_n} \\ &\sim \alpha_{n=0} |\Psi_{n=0}^R\rangle e^{t \text{Im } \mathcal{E}_0} e^{-it \text{Re } \mathcal{E}_0}, \end{aligned} \quad (43)$$

where α_n is the weight for the corresponding state.

C. Case III: Complex eigenvalues and the degenerate quantum states with the maximum imaginary part of all eigenvalues

The NH Hamiltonian $\hat{\mathcal{H}}_{\text{NH}}$ has complex eigenvalues, i.e., $\text{Im } \mathcal{E}_n \neq 0$, and $|\Psi_n^R\rangle$ are m -fold degenerate quantum states with the same maximum imaginary part of all eigenvalues i.e.,

$$\text{Im } \mathcal{E}_n = \Gamma > \text{Im } \mathcal{E}_{m < n < N}, \quad n = 1, 2, \dots, m, m < N.$$

In the limit of $t \rightarrow \infty$, the system reaches a NHTS and we have a subspace from m -fold degenerate quantum states with the same maximum imaginary part of all eigenvalues $|\Psi_n^R\rangle$, $n = 1, 2, \dots, m, m < N$. Using a similar approach, we have

$$\begin{aligned} |\Psi^R\rangle &= \sum_{n=1}^N \alpha_n |\Psi_n^R\rangle e^{-i\mathcal{E}_n t} \\ &= \sum_{n=1}^N \alpha_n |\Psi_n^R\rangle e^{t \text{Im } \mathcal{E}_n} e^{-it \text{Re } \mathcal{E}_n} \\ &\sim e^{t\Gamma} \left(\sum_{n=1}^m \alpha_n |\Psi_n^R\rangle e^{-it \text{Re } \mathcal{E}_n} \right), \end{aligned} \quad (44)$$

where α_n is the weight for the corresponding state.

As a result, for a NHTS, the original NH model is reduced into a subspace of m -fold degenerate quantum states with the same maximum imaginary part of all eigenvalues $|\Psi_n^R\rangle$, $n = 1, 2, \dots, m, m < N$. In the following part, we use a projection operator to characterize the reduction, i.e.,

$$|\Psi^R\rangle \rightarrow \hat{P} |\Psi^R\rangle = |\psi^R\rangle$$

and

$$\hat{\mathcal{H}}_{\text{NH}} \rightarrow \hat{P} \hat{\mathcal{H}}_{\text{NH}} \hat{P}^{-1} = \hat{\mathcal{H}}'_{\text{NH}},$$

where $\hat{\mathcal{H}}'_{\text{NH}}$ and $|\psi^R\rangle$ are the Hamiltonian and quantum state of the subspace, respectively. Now, the density matrix in the NHTS ρ_{NHTS}^S of the original NH Hamiltonian is reduced into $(\rho'_{\text{NHTS}})^S$ of $\hat{\mathcal{H}}'_{\text{NH}}$ in the subspace.

In addition, we show the method to calculate $\hat{\mathcal{H}}'_{\text{NH}}$. First, we define the basis of the original NH system

$$\{ |S_n^R\rangle, \quad n = 1, 2, \dots, N \}.$$

Second, under projection to subspace, we have a projection basis, i.e.,

$$\begin{aligned} \{ |S_n^R\rangle, n = 1, 2, \dots, N \} &\rightarrow \{ \hat{P} |S_n^R\rangle, n = 1, 2, \dots, N \} \\ &= \{ |s_n^R\rangle, n = 1, 2, \dots, m \}. \end{aligned}$$

Third, based on the projection basis $\{|s_j^R\rangle\}$, we derive the effective Hamiltonian

$$\hat{\mathcal{H}}'_{\text{NH}} = \sum_{ij} h_{ij} |s_j^R\rangle\langle s_i^R| + i\Gamma, \quad (45)$$

where $h_{ij} = \langle s_i^R | \hat{\mathcal{H}}_{\text{NH}} |s_j^R\rangle$, $i, j = 1, 2, \dots, m$.

Then, after globally shifting $i\Gamma$, i.e., $\hat{\mathcal{H}}_{\text{NH}} \rightarrow \hat{\mathcal{H}}_{\text{NH}} - i\Gamma$ or $\hat{\mathcal{H}}'_{\text{NH}} \rightarrow \hat{\mathcal{H}}'_{\text{NH}} - i\Gamma$, the situation is mapped to Case I. Finally, the density matrix in the NHTS is obtained as

$$(\rho'_{\text{NHTS}})^S = \hat{S}'(e^{-\beta_T \hat{\mathcal{H}}'_0})(\hat{S}')^\dagger = e^{-\beta_T \hat{\mathcal{H}}_L}, \quad (46)$$

TABLE I. The density matrix in non-Hermitian thermal states for an arbitrary non-Hermitian system with finite temperature T .

All real eigenvalues	Complex eigenvalues	
$\rho_{\text{NHTS}}^S = \hat{S}(e^{-\beta_T \hat{H}_0})\hat{S}^\dagger = e^{-\beta_T \hat{H}_L}$	Nondegenerate $\rho_{\text{NHTS}}^S = \Psi_0^R\rangle\langle\Psi_0^R $	Degenerate $(\rho_{\text{NHTS}}^S)^S = \hat{S}'(e^{-\beta_T \hat{H}'_0})(\hat{S}')^\dagger = e^{-\beta_T \hat{H}_L}$

where $\hat{H}'_0 = (\hat{S}')^{-1}\hat{H}'_{\text{NH}}\hat{S}'$ [$\hat{H}'_0 = (\hat{H}'_0)^\dagger$] and

$$\hat{S}' = \hat{P}\hat{S}\hat{P}^{-1} = \left(\sum_{n=1}^m |\psi_n^R\rangle\langle\psi_n^R| \right)^{\frac{1}{2}}. \quad (47)$$

In summary, the quantum Liouvillian statistical theory for an arbitrary NH system with finite- T can be expressed in Table I.

VI. THERMODYNAMIC PROPERTIES OF THE THERMAL \mathcal{PT} SYSTEM

Using the quantum Liouvillian statistical theory, we study thermodynamic properties for the NHTSs ρ_{NHTS}^S of the thermal \mathcal{PT} system.

Now, the physical properties of the original NH system \hat{H}_{NH} at finite- T correspond to those of a Hermitian system of LH, \hat{H}_L . According to $e^{-\beta_T \hat{H}_L} = \hat{S}(e^{-\beta_T \hat{H}_0})\hat{S}^\dagger$, we obtain the analytical result as

$$e^{-\beta_T \hat{H}_L} = \sigma_x A + \sigma_z B + \hat{I} C, \quad (48)$$

where

$$\begin{aligned} A &= -\sinh(\beta_T \sqrt{h^2 - \gamma^2}), \\ B &= \sinh(\beta_{\text{NH}}) \cdot \cosh(\beta_T \sqrt{h^2 - \gamma^2}), \\ C &= \cosh(\beta_{\text{NH}}) \cdot \cosh(\beta_T \sqrt{h^2 - \gamma^2}), \end{aligned} \quad (49)$$

and $\hat{I} = \begin{pmatrix} 1 & 0 \\ 0 & -1 \end{pmatrix}$. From the generalized Baker–Campbell–Hausdorff formulation, the LH is derived as

$$\hat{H}_L = -\frac{1}{\beta_T} \frac{\cosh^{-1} C}{|\vec{r}_{\text{eff}}|} (\vec{\sigma} \cdot \vec{r}_{\text{eff}}), \quad (50)$$

where $\vec{\sigma} = (\sigma_x, \sigma_y, \sigma_z)$, $\vec{r}_{\text{eff}} = (A, 0, B)$, and $|\vec{r}_{\text{eff}}| = \sqrt{A^2 + B^2}$. See the detailed calculations about the generalized Baker–Campbell–Hausdorff formulation in Appendix B. After diagonalizing \hat{H}_L , the Liouvillian energy levels (the eigenvalues for \hat{H}_L) are

$$E_{\pm}^L = \pm \frac{1}{\beta_T} \cosh^{-1} [\cosh \beta_{\text{NH}} \cdot \cosh(\beta_T \sqrt{h^2 - \gamma^2})], \quad (51)$$

which are quite different from the energy levels (the eigenvalues for \hat{H}_{NH}) $E_{\pm} = \pm \sqrt{h^2 - \gamma^2}$, as shown in Fig. 4. As a result, the Liouvillian energy gap is

$$\Delta = 2|E_{\pm}^L| = \frac{2}{\beta_T} \cosh^{-1} [\cosh \beta_{\text{NH}} \cdot \cosh(\beta_T \sqrt{h^2 - \gamma^2})]. \quad (52)$$

At the EP, Δ diverges, i.e., when $\beta_{\text{NH}} \rightarrow \infty$, $\Delta \rightarrow \infty$. Remember the energy gap for \hat{H}_{NH} at EP turns to zero, i.e., when $\beta_{\text{NH}} \rightarrow \infty$, $\omega_0 = 2\sqrt{h^2 - \gamma^2} \rightarrow 0$. According to LBZ law,

we have

$$P_n = \frac{1}{Z_{\text{NHTS}}^S} \exp \left[\frac{\cosh^{-1} C}{|\vec{r}_{\text{eff}}|} (\vec{\sigma} \cdot \vec{r}_{\text{eff}}) \right]. \quad (53)$$

The expected values of spin operators σ_i ($i = x, y, z$) are defined as

$$n_i = \langle \sigma_i \rangle = \frac{1}{Z_{\text{NHTS}}^S} \text{Tr}(\sigma_i \cdot e^{-\beta_T \hat{H}_L}). \quad (54)$$

After straightforward calculations, we have

$$\begin{aligned} \vec{n} &= (n_x, n_y, n_z) = \left(\frac{A}{C}, 0, \frac{B}{C} \right) \\ &= \left(\frac{-\tanh(\beta_T \sqrt{h^2 - \gamma^2})}{\cosh \beta_{\text{NH}}}, 0, \tanh \beta_{\text{NH}} \right) \end{aligned} \quad (55)$$

in the region of $h > \gamma$ [50]. Figure 5(a) shows the results of \vec{n} . Based on these results, when β_{NH} increases from zero to infinite, the spin direction changes from the x direction to the z direction. Figures 5(b) to 5(d) show the behavior of $n_i = \langle \sigma_i \rangle$ at $T = 10$, respectively. Approaching EP $h \rightarrow \gamma$ (or $\beta_{\text{NH}} \rightarrow \infty$), we have $\hat{H}_L \rightarrow -\frac{\beta_{\text{NH}}}{\beta_T} \sigma_z$ at finite- T . The external field $|\frac{\beta_{\text{NH}}}{\beta_T}|$ in LH \hat{H}_L becomes *infinite*. As a result, \vec{n} is fixed to be polarized along the z direction with saturated amplitude 1 [see the magenta arrows marked by a magenta line in Fig. 5(a)]. On the other hand, for the region of $h < \gamma$, the NHTS becomes a pure state described by $|\Psi_+^R\rangle$ and we have

$$\vec{n} = \left(0, -\sqrt{1 - \left(\frac{h}{\gamma} \right)^2}, \frac{h}{\gamma} \right). \quad (56)$$

As shown in Fig. 5(a), the red arrows (the expected values of σ_i) swerve from the z direction to the y direction with increasing γ . In Fig. 5(d), we can see that, as the temperature T approaches infinity, n_z is not 0 in the phase with \mathcal{PT} symmetry

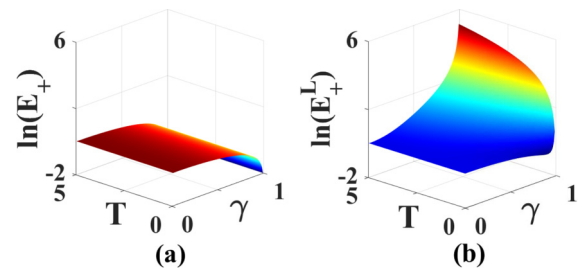


FIG. 4. (a) The energy level $E_+ = \sqrt{h^2 - \gamma^2}$ versus temperature T and γ for the non-Hermitian Hamiltonian \hat{H}_{NH} . (b) The Liouvillian energy level $E_+^L = \frac{1}{\beta_T} \cosh^{-1} [\cosh \beta_{\text{NH}} \cdot \cosh(\beta_T \sqrt{h^2 - \gamma^2})]$ versus temperature T and γ for the Liouvillian Hamiltonian \hat{H}_L .

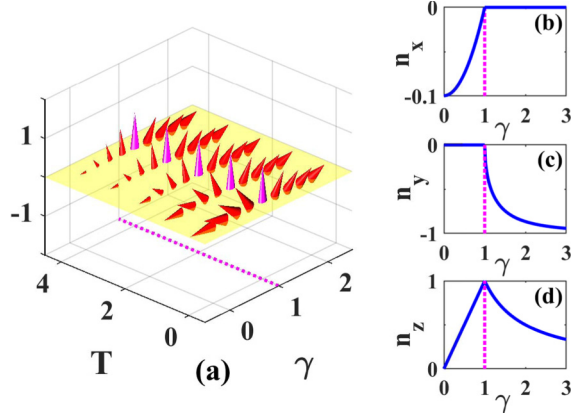


FIG. 5. (a) Expected values $n_i = \langle \sigma_i \rangle$ of the spin operator from Liouvillian-Boltzmann distribution for the non-Hermitian thermal states ρ_{NHTS}^S of the thermal \mathcal{PT} system. (b), (c), and (d) depict n_x , n_y , n_z at temperature $T = 10$, respectively.

($h > \gamma$), which means the nonthermalization occurs in a high temperature.

From the above discussions, we conclude that $n_i = \langle \sigma_i \rangle$ is always continuous when crossing over the EP. Furthermore, we calculate $\frac{\partial \bar{n}}{\partial \gamma}$. Because $h = \gamma$ is a transition from real spectra to complex, the NHTSs of both sides ($h > \gamma$ and $h < \gamma$) are described by different functions. After straightforward calculation, we can see

$$\frac{\partial \bar{n}}{\partial \gamma} = \left\{ \begin{array}{l} \frac{\gamma}{h\sqrt{h^2 - \gamma^2}} \tanh(\beta_T \sqrt{h^2 - \gamma^2}) \\ + \frac{\gamma \beta_T}{h} [1 - \tanh^2(\beta_T \sqrt{h^2 - \gamma^2})], 0, \frac{1}{h} \end{array} \right\}, \quad (57)$$

$$\frac{\partial \bar{n}}{\partial T} = \left\{ \begin{array}{l} \frac{\sqrt{h^2 - \gamma^2}}{k_B T^2 \cosh \beta_{\text{NH}}} [1 - \tanh^2(\beta_T \sqrt{h^2 - \gamma^2})], 0, 0 \end{array} \right\} \quad (58)$$

for $h > \gamma$ and

$$\frac{\partial \bar{n}}{\partial \gamma} = \left(0, -\frac{1}{\sqrt{1 - (\frac{h}{\gamma})^2}} \frac{h^2}{\gamma^3}, -\frac{h}{\gamma^2} \right) \quad (59)$$

for $h < \gamma$.

Figure 6 shows the result of $\frac{\partial \bar{n}}{\partial \gamma}$. We can see that $\frac{\partial n_x}{\partial \gamma}$ depends on γ and temperature T , and $\frac{\partial n_y}{\partial \gamma}$ and $\frac{\partial n_z}{\partial \gamma}$ depend only on γ . Moreover, at finite-T $T \neq 0$, $\frac{\partial \bar{n}}{\partial \gamma}$ is discontinued at the $\gamma = h$. It means a ‘‘second-order’’ phase transition at the EP: there exists a $\nu = \frac{1}{2}$ critical rule for $\frac{\partial \bar{n}}{\partial \gamma}$: at finite-T $T \neq 0$,

$$\frac{\partial \bar{n}}{\partial \gamma} = (2\beta_T, 0, h^{-1}) \quad (60)$$

for $h \rightarrow \gamma + 0^+$ in the phase with \mathcal{PT} symmetry ($h \geq \gamma$) and

$$\frac{\partial \bar{n}}{\partial \gamma} = (0, -(2h)^{-\frac{1}{2}}(\gamma - h)^{-\nu}, -\gamma^{-1}) \quad (61)$$

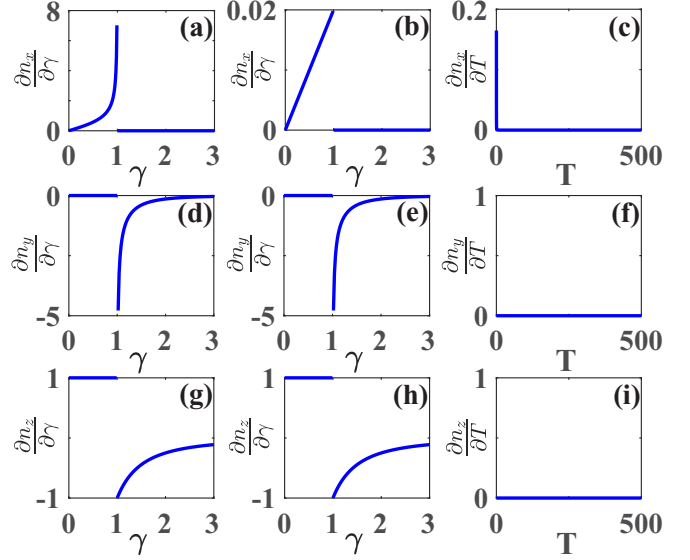


FIG. 6. The derivatives of expected values of the spin operators of the thermal \mathcal{PT} system versus γ or temperature T . (a), (d), and (g) are $\frac{\partial \bar{n}}{\partial \gamma}$ versus γ at the temperature $T = 0.01$, respectively. (b), (e), and (h) are $\frac{\partial \bar{n}}{\partial \gamma}$ versus γ at the temperature $T = 100$, respectively. (c), (f), and (i) are $\frac{\partial \bar{n}}{\partial T}$ versus temperature T at $\gamma = 0.999$, respectively.

for $\gamma \rightarrow h + 0^+$ in the phase with \mathcal{PT} -symmetry breaking ($h < \gamma$); while at zero temperature $T = 0$,

$$\frac{\partial \bar{n}}{\partial \gamma} = ((2h)^{-\frac{1}{2}}(h - \gamma)^{-\nu}, 0, h^{-1}) \quad (62)$$

for $h \rightarrow \gamma + 0^+$ and

$$\frac{\partial \bar{n}}{\partial \gamma} = (0, -(2h)^{-\frac{1}{2}}(\gamma - h)^{-\nu}, -\gamma^{-1}) \quad (63)$$

for $\gamma \rightarrow h + 0^+$. To emphasize the strangeness of the $\nu = \frac{1}{2}$ critical rule, we call it *zero temperature anomaly* for the thermodynamic phase transition at the EP.

VII. CONCLUSION

In this paper, we study \mathcal{PT} -symmetric NH quantum systems at finite-T and develop a quantum Liouvillian statistical theory for NH systems at finite-T. By considering a controllable open quantum system S coupling with two separate environments B and E , we design a thermal \mathcal{PT} system and solve the corresponding GKSL master equation to find the correct distribution. In addition, we define the NHTS for NH systems at finite-T and explore its physical properties. As a result, in general, the usual BZ law and the Equal Probability Principle are all no longer valid for the NH system at finite-T. Instead, the usual BZ law $P_n \sim e^{-\mathcal{E}_n/k_B T}$ is replaced by the LBZ law $P_n \sim e^{-\mathcal{E}_n^L/k_B T}$, where \mathcal{E}_n^L is a Liouvillian energy level of $\hat{\mathcal{H}}_L$ rather than an energy level \mathcal{E}_n of $\hat{\mathcal{H}}_{\text{NH}}$. Based on the quantum Liouvillian statistical theory, we derive analytical results of thermodynamic properties for the thermal \mathcal{PT} system and find that a ‘‘continuous’’ thermodynamic phase transition occurs at the EP, where a

zero-temperature anomaly exists. Therefore, the quantum Liouillian statistical theory provides the necessary method to study NH many-body physics and hence can be used to deal with NH quantum many-body problems, including the topological property, transport property, correlation property, and so on. In the future, we will study more complex NH models and explore the possible exotic phenomena in NH systems at finite-T.

ACKNOWLEDGMENTS

This work was supported by the Natural Science Foundation of China (Grants No. 11974053 and No. 12174030). We are grateful to Wei Yi, Shu Chen, Gao-Yong Sun, Lin-Hu Li, Yi-Bin Guo, Xue-Xi Yi, and Ching-Hua Lee for helpful discussions that contributed to clarifying some aspects related to the present work.

APPENDIX A: QUANTUM MASTER EQUATION OF THE OPEN NON-HERMITIAN QUANTUM SYSTEM

For the total system $S + B + E$, we trace out E from it and get the GKSL equation of the reduced density matrix ρ^{S+B}

$$\frac{d\rho^{S+B}}{dt} = -i[\hat{H}_{S+B}, \rho^{S+B}] - \frac{1}{2}\{\hat{L}_{ES}^\dagger \hat{L}_{ES}, \rho^{S+B}\} + \hat{L}_{ES} \rho^{S+B} \hat{L}_{ES}^\dagger. \quad (\text{A1})$$

We make the postselection measurement for the number of particles $\hat{N} = (c_1^\dagger c_1 + c_2^\dagger c_2) \otimes \hat{I}_B$ in S , so that it is always $N = 1$ [44]. After the postselection measurements, the quantum jumping term $\hat{L}_{ES} \rho^{S+B} \hat{L}_{ES}^\dagger$ will be projected out [45]. Then we get Eq. (17).

In general, the derivation of a quantum Markovian master equation is performed in the interaction picture. Thus, we write Eq. (17) as in the interaction picture

$$\frac{d}{dt} \rho_{In}^{S+B}(t) = -i(\hat{V}_{In}(t) \rho_{In}^{S+B}(t) - \rho_{In}^{S+B}(t) \hat{V}_{In}^\dagger(t)), \quad (\text{A2})$$

where

$$\rho_{In}^{S+B}(t) = e^{i\hat{H}_{\text{eff},0}t} \rho^{S+B}(t) e^{-i\hat{H}_{\text{eff},0}^\dagger t}, \quad (\text{A3})$$

$$\hat{V}_{In}(t) = e^{i\hat{H}_{\text{eff},0}t} \hat{H}_{BS} e^{-i\hat{H}_{\text{eff},0}t}, \quad (\text{A4})$$

and

$$\hat{H}_{\text{eff},0} = \hat{H}_{\text{NH}} \otimes \hat{I}_B + \hat{I}_S \otimes \hat{H}_B. \quad (\text{A5})$$

For simplicity, we use $[A, B]_\dagger$ to denote $AB - BA^\dagger$. So $\frac{d}{dt} \rho_{In}^{S+B}(t) = -i[\hat{V}_{In}(t), \rho_{In}^{S+B}(t)]_\dagger$. Its equivalent integral form is

$$\rho_{In}^{S+B}(t) = \rho_{In}^{S+B}(0) - i \int_0^t ds [\hat{V}_{In}(s), \rho_{In}^{S+B}(s)]_\dagger. \quad (\text{A6})$$

Combining Eqs. (A2) and (A6), and taking the partial trace over the degrees of freedom of the environment B , we give the reduced density matrix $\rho_{In}^S(t)$ in the subsystem S

$$\frac{d}{dt} \rho_{In}^S(t) = -i \text{Tr}_B [\hat{V}_{In}(t), \rho_{In}^{S+B}(0)]_\dagger - \int_0^t ds \text{Tr}_B [\hat{V}_{In}(t), [\hat{V}_{In}(s), \rho_{In}^{S+B}(s)]_\dagger]_\dagger. \quad (\text{A7})$$

Here, we assume $\text{Tr}_B [\hat{V}_{In}(t), \rho_{In}^{S+B}(0)]_\dagger = 0$ [43]. Additionally, we use the Born approximation that the subsystem S has little influence on the environment B , so $\rho_{In}^{S+B}(s) \sim \rho_{In}^S(s) \otimes \rho_{In}^B$. By the Markov approximation $\rho_{In}^S(s) \sim \rho_{In}^S(t)$, we have

$$\frac{d}{dt} \rho_{In}^S(t) = - \int_0^t ds \text{Tr}_B [\hat{V}_{In}(t), [\hat{V}_{In}(s), \rho_{In}^S(t) \otimes \rho_{In}^B]_\dagger]_\dagger. \quad (\text{A8})$$

We substitute s by $t - s$, the above equation can be expressed as

$$\frac{d}{dt} \rho_{In}^S(t) = \text{Tr}_B \int_0^t ds [\hat{V}_{In}(t-s) \rho_{In}^S(t) \otimes \rho_{In}^B \hat{V}_{In}^\dagger(t) - \hat{V}_{In}(t) \hat{V}_{In}(t-s) \rho_{In}^S(t) \otimes \rho_{In}^B] + \text{H.c.} \quad (\text{A9})$$

Using eigenstates of \hat{H}_{NH} in $\hbar > \gamma$, we insert the identity operator $\hat{I} = \sum_{m=\pm} |m\rangle_R \langle m|_L \otimes \hat{I}_B$ in $\hat{V}_{In}(t)$ and get

$$\begin{aligned} \hat{V}_{In}(t) &= e^{i\hat{H}_{\text{eff},0}t} \left[\sum_a \sum_{m=\pm} |m\rangle_R \langle m|_L \gamma_a c_a^\dagger c_a \sum_{n=\pm} |n\rangle_R \langle n|_L \otimes \hat{B}_a(t) \right] e^{-i\hat{H}_{\text{eff},0}t} \\ &= \sum_a \sum_{m=\pm} \sum_{n=\pm} e^{iE_m t} |m\rangle_R \langle m|_L \gamma_a c_a^\dagger c_a |n\rangle_R \langle n|_L e^{-iE_n t} \otimes \hat{B}_a(t) \\ &= \sum_a \sum_{m=\pm} \sum_{\omega} e^{-i\omega t} |m\rangle_R \langle m|_L \gamma_a c_a^\dagger c_a |m+\omega\rangle_R \langle m+\omega|_L \otimes \hat{B}_a(t), \end{aligned} \quad (\text{A10})$$

where $|m\rangle_{R,L}$ are the right or left eigenstates of \hat{H}_{NH} with the eigenvalue E_m , and $|n\rangle_{R,L} = |m+\omega\rangle_{R,L}$ are the eigenvalues \hat{H}_{NH} with the eigenvalue $E_{m+\omega}$ and they satisfy ${}_L \langle m|m\rangle_R = 1$. In addition, we have $\omega = \pm\omega_0$, 0 with $\omega_0 = |E_+ - E_-| = 2\sqrt{\hbar^2 - \gamma^2}$.

We define an operator $\hat{A}_a(\omega)$,

$$\hat{A}_a(\omega) = \sum_{m=\pm} |m\rangle_R \langle m|_L \gamma_a c_a^\dagger c_a |m+\omega\rangle_R \langle m+\omega|_L \quad (\text{A11})$$

with $a = 1$ or 2 . Now, $\hat{V}_{In}(t)$ is written as

$$\hat{V}_{In}(t) = \sum_a \sum_\omega e^{-i\omega t} \hat{A}_a(\omega) \otimes \hat{B}_a(t). \quad (\text{A12})$$

Substituting this form of $\hat{V}_{In}(t)$ to Eq. (A9), we get

$$\begin{aligned} \frac{d}{dt} \rho_{In}^S(t) &= \sum_b \sum_\omega \sum_a \sum_{\omega_1} e^{i(\omega_1 - \omega)t} \hat{A}_b(\omega) \rho_{In}^S(t) \hat{A}_a^\dagger(\omega_1) \int_0^t ds e^{i\omega s} \text{Tr}_B(\hat{B}_b(t-s) \rho_{In}^B \hat{B}_a^\dagger(t)) \\ &\quad - \sum_a \sum_{-\omega_1} \sum_b \sum_\omega e^{i(\omega_1 - \omega)t} \hat{A}_a(-\omega_1) \hat{A}_b(\omega) \rho_{In}^S(t) \int_0^t ds e^{i\omega s} \text{Tr}_B(\hat{B}_a^\dagger(t) \hat{B}_b(t-s) \rho_{In}^B) \\ &\quad + \sum_a \sum_{\omega_1} \sum_b \sum_\omega e^{-i(\omega_1 - \omega)t} \hat{A}_a(\omega_1) \rho_{In}^S(t) \hat{A}_b^\dagger(\omega) \int_0^t ds e^{-i\omega s} \text{Tr}_B(\rho_{In}^B \hat{B}_b^\dagger(t-s) \hat{B}_a(t)) \\ &\quad - \sum_b \sum_\omega \sum_a \sum_{-\omega_1} e^{-i(\omega_1 - \omega)t} \rho_{In}^S(t) \hat{A}_b^\dagger(\omega) \hat{A}_a^\dagger(-\omega_1) \int_0^t ds e^{-i\omega s} \text{Tr}_B(\rho_{In}^B \hat{B}_b^\dagger(t-s) \hat{B}_a(t)). \end{aligned} \quad (\text{A13})$$

We employ the one-sided Fourier transforms

$$\begin{aligned} \Gamma_{ab}(\omega) &= \int_0^t ds e^{i\omega s} \langle \hat{B}_a^\dagger(s) \hat{B}_b(0) \rangle, \\ \Gamma_{ba}^*(\omega) &= \int_0^t ds e^{-i\omega s} \langle \hat{B}_b^\dagger(0) \hat{B}_a(s) \rangle \end{aligned} \quad (\text{A14})$$

of the reservoir correlation functions $\langle \hat{B}_a^\dagger(s) \hat{B}_b(0) \rangle = \text{Tr}_B(\hat{B}_a^\dagger(t) \hat{B}_b(t-s) \rho_{In}^B)$ of the environment B to simply Eq. (A13) equation. Eventually, $\frac{d}{dt} \rho_{In}^S(t)$ of the subsystem S in the interaction picture is

$$\begin{aligned} \frac{d}{dt} \rho_{In}^S(t) &= \sum_{a,b} \sum_\omega \sum_{\omega_1} e^{i(\omega_1 - \omega)t} \Gamma_{ab}(\omega) (\hat{A}_b(\omega) \rho_{In}^S(t) \hat{A}_a^\dagger(\omega_1) \\ &\quad - \hat{A}_a(-\omega_1) \hat{A}_b(\omega) \rho_{In}^S(t)) \\ &\quad + \sum_{a,b} \sum_\omega \sum_{\omega_1} e^{-i(\omega_1 - \omega)t} \Gamma_{ba}^*(\omega) (\hat{A}_a(\omega_1) \rho_{In}^S(t) \hat{A}_b^\dagger(\omega) \\ &\quad - \rho_{In}^S(t) \hat{A}_b^\dagger(\omega) \hat{A}_a^\dagger(-\omega_1)). \end{aligned} \quad (\text{A15})$$

We use the rotating wave approximation to average out the high-frequency part of the quantum transition processes and ignore the case of $\omega \neq \omega_1$, then get

$$\begin{aligned} \frac{d}{dt} \rho_{In}^S(t) &= \sum_{a,b} \sum_\omega [\Gamma_{ab}(\omega) (\hat{A}_b(\omega) \rho_{In}^S(t) \hat{A}_a^\dagger(\omega) \\ &\quad - \hat{A}_a(-\omega) \hat{A}_b(\omega) \rho_{In}^S(t)) + \text{H.c.}] \end{aligned} \quad (\text{A16})$$

The imaginary part of Γ_{ab} only provides a shift of energy levels and does not affect the possible thermodynamic equilibrium state, so we ignore its imaginary part and get $\Gamma_{ab} = \frac{1}{2} \gamma_{ab}$, where $\gamma_{ab} = \int_{-\infty}^{\infty} ds e^{i\omega s} \langle \hat{B}_a^\dagger(s) \hat{B}_b(0) \rangle$ is the real part of Γ_{ab} . Using the Kubo-Martin-Schwinger (KMS) condition $\langle \hat{B}_a^\dagger(t) \hat{B}_b(0) \rangle = \langle \hat{B}_b(0) \hat{B}_a^\dagger(t + i\frac{1}{T}) \rangle$ [43,51], we derive the

temperature-dependent behavior of γ_{ab} ,

$$\gamma_{ab}(-\omega) = e^{-\omega/k_B T} \gamma_{ba}(\omega). \quad (\text{A17})$$

For the sake of simplicity, we use $\begin{pmatrix} A & B \\ C & D \end{pmatrix}$ to denote $\rho_{In}^S(t)$. According to $\frac{d\rho_{In}^S(t)}{dt} = \mathcal{L} \rho_{In}^S(t)$ and $\rho_{In}^S(t) = \begin{pmatrix} A & B \\ C & D \end{pmatrix}$, we get

$$\begin{aligned} \frac{dA}{dt} &= -\gamma_0(1 + e^{\omega_0/k_B T})A + \gamma_0(1 + e^{\omega_0/k_B T}) \frac{h + \gamma}{h - \gamma} D, \\ \frac{dB}{dt} &= -2\gamma_0(e^{\omega_0/k_B T} - 1) \sqrt{\frac{h - \gamma}{h + \gamma}} A - 3\gamma_0(1 + e^{\omega_0/k_B T})B \\ &\quad - \gamma_0(1 + e^{\omega_0/k_B T})C - 2\gamma_0(e^{\omega_0/k_B T} - 1) \sqrt{\frac{h + \gamma}{h - \gamma}} D, \\ \frac{dC}{dt} &= -2\gamma_0(e^{\omega_0/k_B T} - 1) \sqrt{\frac{h - \gamma}{h + \gamma}} A - \gamma_0(1 + e^{\omega_0/k_B T})B \\ &\quad - 3\gamma_0(1 + e^{\omega_0/k_B T})C - 2\gamma_0(e^{\omega_0/k_B T} - 1) \sqrt{\frac{h + \gamma}{h - \gamma}} D, \\ \frac{dD}{dt} &= \gamma_0(1 + e^{\omega_0/k_B T}) \frac{h - \gamma}{h + \gamma} A - \gamma_0(1 + e^{\omega_0/k_B T})D. \end{aligned} \quad (\text{A18})$$

Then we simply and get Eq. (25).

APPENDIX B: GENERALIZED BAKER-CAMPBELL-HAUSDORFF FORMULATION

Generalized Baker-Campbell-Hausdorff formulation: For the case of $\sigma_1^2 = 1$ and $\sigma_2^2 = 1$, we have the following equation:

$$\rho = e^{\vec{r}_1 \cdot \vec{\sigma}} \cdot e^{\vec{r}_2 \cdot \vec{\sigma}} \cdot e^{\vec{r}_1 \cdot \vec{\sigma}} = \alpha + |\vec{r}_{\text{eff}}| \cdot \sigma_{\text{eff}} = e^{c + \vec{r} \cdot \vec{\sigma}}, \quad (\text{B1})$$

where

$$c = \frac{1}{2} \ln(\alpha^2 - |\vec{r}_{\text{eff}}|^2), \quad (\text{B2})$$

and

$$|\vec{r}| = \tanh^{-1} \left(\frac{|\vec{r}_{\text{eff}}|}{\alpha} \right), \quad (\text{B3})$$

with

$$\alpha = \cosh(2r_1) \cdot \cosh r_2 + (\vec{n}_1 \cdot \vec{n}_2) \sinh(2r_1) \cdot \sinh r_2,$$

$$|\vec{r}_{\text{eff}}| = \{[\sinh(2r_1) \cdot \cosh r_2 + 2(\vec{n}_1 \cdot \vec{n}_2) \sinh^2 r_1 \cdot \sinh r_2]^2 + (\sinh r_2)^2\}^{1/2},$$

$$\sigma_{\text{eff}} = |\vec{r}_{\text{eff}}|^{-1} \cdot \{\sigma_1[\sinh(2r_1) \cdot \cosh r_2 + 2(\vec{n}_1 \cdot \vec{n}_2) \sinh^2 r_1 \cdot \sinh r_2] + \sigma_2 \sinh r_2\},$$

$$r_1 = |\vec{r}_1| \text{ and } r_2 = |\vec{r}_2|.$$

We then prove the above generalized Baker-Campbell-Hausdorff formulation.

First, for $\sigma_n^2 = 1$, we have

$$e^{\vec{r} \cdot \vec{\sigma}} = \cosh r + \sigma_n \sinh r, \quad (\text{B4})$$

where $|\vec{r}| = r$ with $\cosh^2 r - \sinh^2 r = 1$ and $\sigma_n = \frac{\vec{r} \cdot \vec{\sigma}}{r}$. On the other hand, for the case of $X = d + \vec{f} \cdot \vec{\sigma}$ with $f = |\vec{f}|$, we have $X = e^{c + \vec{r} \cdot \vec{\sigma}}$, where

$$e^c \cosh r = d, \quad e^c \sinh r = f. \quad (\text{B5})$$

Then, we have $r = \tanh^{-1}(\frac{f}{d})$ and $c = \frac{1}{2} \ln(d^2 - f^2)$.

Next, we calculate $\rho = e^{\vec{r}_1 \cdot \vec{\sigma}} \cdot e^{\vec{r}_2 \cdot \vec{\sigma}} \cdot e^{\vec{r}_1 \cdot \vec{\sigma}}$ and get

$$\begin{aligned} \rho &= e^{\vec{r}_1 \cdot \vec{\sigma}} \cdot e^{\vec{r}_2 \cdot \vec{\sigma}} \cdot e^{\vec{r}_1 \cdot \vec{\sigma}} \\ &= (\cosh r_1 + \sigma_1 \sinh r_1) \\ &\quad \times (\cosh r_2 + \sigma_2 \sinh r_2) \\ &\quad \times (\cosh r_1 + \sigma_1 \sinh r_1), \end{aligned} \quad (\text{B6})$$

where $r_1 = |\vec{r}_1|$ and $r_2 = |\vec{r}_2|$. The result is obtained as

$$\begin{aligned} \rho &= (\cosh r_1 \cdot \cosh r_2 + \sigma_1 \sinh r_1 \cdot \cosh r_2 \\ &\quad + \sigma_2 \cosh r_1 \cdot \sinh r_2 + \sigma_1 \sigma_2 \sinh r_1 \cdot \sinh r_2) \\ &\quad \times (\cosh r_1 + \sigma_1 \sinh r_1) \\ &= \cosh(2r_1) \cdot \cosh r_2 + (\vec{n}_1 \cdot \vec{n}_2) \sinh(2r_1) \cdot \sinh r_2 \\ &\quad + \sigma_1[\sinh(2r_1) \cdot \cosh r_2 + 2(\vec{n}_1 \cdot \vec{n}_2) \sinh^2 r_1 \cdot \sinh r_2] \\ &\quad + \sigma_2 \sinh r_2, \end{aligned} \quad (\text{B7})$$

where $\vec{n}_1 = \frac{\vec{r}_1}{|\vec{r}_1|}$ and $\vec{n}_2 = \frac{\vec{r}_2}{|\vec{r}_2|}$. Here, we used $\{\sigma_1, \sigma_2\} = 2(\vec{n}_1 \cdot \vec{n}_2)$.

Third, we show the final result:

$$\rho = \alpha + |\vec{r}_{\text{eff}}| \cdot \sigma_{\text{eff}} = e^{c + \vec{r} \cdot \vec{\sigma}}, \quad (\text{B8})$$

where

$$c = \frac{1}{2} \ln(\alpha^2 - |\vec{r}_{\text{eff}}|^2), \quad r = \tanh^{-1} \left(\frac{|\vec{r}_{\text{eff}}|}{\alpha} \right),$$

with $\alpha = \cosh 2r_1 \cdot \cosh r_2 + (\vec{n}_1 \cdot \vec{n}_2) \sinh 2r_1 \cdot \sinh r_2$,

$$|\vec{r}_{\text{eff}}| = \{[\sinh(2r_1) \cdot \cosh r_2 + 2(\vec{n}_1 \cdot \vec{n}_2) \sinh^2 r_1 \cdot \sinh r_2]^2 + (\sinh r_2)^2\}^{1/2}$$

and

$$\begin{aligned} \sigma_{\text{eff}} &= |\vec{r}_{\text{eff}}|^{-1} \cdot \{\sigma_1[\sinh(2r_1) \cdot \cosh r_2 \\ &\quad + 2(\vec{n}_1 \cdot \vec{n}_2) \sinh^2 r_1 \cdot \sinh r_2] + \sigma_2 \sinh r_2\}. \end{aligned}$$

In general, according to $\alpha^2 - |\vec{r}_{\text{eff}}|^2 = 1$, we have

$$c = \frac{1}{2} \ln(\alpha^2 - |\vec{r}_{\text{eff}}|^2) \equiv 0. \quad (\text{B9})$$

So

$$\rho = e^{\frac{\cosh^{-1} \alpha}{|\vec{r}_{\text{eff}}|} (\vec{\sigma} \cdot \vec{r}_{\text{eff}})} = e^{\cosh^{-1} \alpha \cdot \sigma_{\text{eff}}}. \quad (\text{B10})$$

APPENDIX C: EXPECTED VALUES OF THE SPIN OPERATORS IN THE \mathcal{PT} SYSTEM FOR THE TWO CHOICES

1. Choice I

In choice I, the expected values of physical operators σ_i ($i = x, y, z$) of the thermal \mathcal{PT} system are

$$n_i = \langle \sigma_i \rangle = \frac{1}{Z^I} \text{Tr}(\sigma_i \cdot \rho^I), \quad (\text{C1})$$

where $Z^I = \text{Tr}(\rho^I)$. It is obvious that $Z^I = Z_0$, where $Z_0 = \text{Tr}(\rho_0)$ is the partition function for Hermitian model \hat{H}_0

According to the definition of $\rho^I = \hat{S} \rho_0 \hat{S}^{-1}$, we have

$$\rho^I = C \hat{I} + \sigma_x A + \sigma_y B \quad (\text{C2})$$

for the thermal \mathcal{PT} system, where $\hat{I} = \begin{pmatrix} 1 & 0 \\ 0 & 1 \end{pmatrix}$ and

$$\begin{aligned} A &= -\cosh \beta_{\text{NH}} \cdot \sinh(\beta_T \sqrt{h^2 - \gamma^2}), \\ B &= -i \sinh \beta_{\text{NH}} \cdot \sinh(\beta_T \sqrt{h^2 - \gamma^2}), \\ C &= \cosh(\beta_T \sqrt{h^2 - \gamma^2}). \end{aligned} \quad (\text{C3})$$

We obtain the expected values of σ_x , σ_y , and σ_z as

$$\begin{aligned} n_x &= \frac{A}{C} = -\cosh \beta_{\text{NH}} \cdot \tanh(\beta_T \sqrt{h^2 - \gamma^2}), \\ n_y &= \frac{B}{C} = -i \sinh \beta_{\text{NH}} \cdot \tanh(\beta_T \sqrt{h^2 - \gamma^2}), \\ n_z &= 0. \end{aligned} \quad (\text{C4})$$

We can see that the expected value of σ_y becomes imaginary, i.e., $n_y \neq (n_y)^*$, which means that the result is unphysical.

At $\gamma = 0$, the Hamiltonian of the thermal \mathcal{PT} system becomes a Hermitian Hamiltonian $\hat{H} = h\sigma_x$, which corresponds to the Hermitian case. In this case, different quantum states at the thermal equilibrium state obey the BZ distribution law, i.e., $P_+ = e^{-\beta_T E_+}$ and $P_- = e^{-\beta_T E_-}$, where $E_{\pm} = \pm h$ are energy levels. In Fig. 7(a), the blue curve and blue triangles represent the expected values of σ_x from choice I ρ^I and those derived by directly solving the GKSL equation ρ_{NHTS}^S in the Hermitian case ($\gamma = 0$), respectively. Except for the case of $\gamma = 0$, the others correspond to the NH case, such as the case of $\gamma = 0.9$ marked by the red curve and red triangles in Fig. 7(a). The

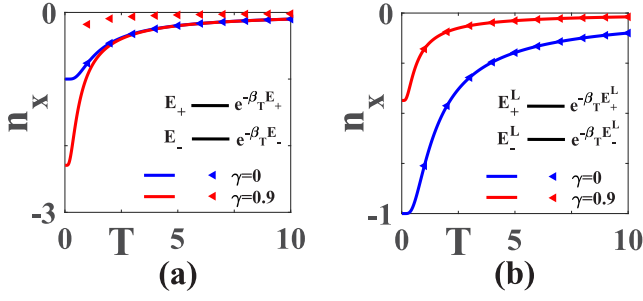


FIG. 7. The expected value $\langle \sigma_x \rangle = n_x$ of the spin operator in the thermal \mathcal{PT} system versus the temperature T for $\gamma = 0$ (Hermitian case) and $\gamma = 0.9$ (non-Hermitian case). (a) The comparison between the results from choice I ρ^I (solid curves) and those obtained by directly solving the Gorini-Kossakowski-Sudarshan-Lindblad equation (the small triangles). (b) The comparison between the results from choice II ρ^{II} (solid curves) and those derived by directly solving the Gorini-Kossakowski-Sudarshan-Lindblad equation (the small triangles).

results of n_x derived by ρ^I (the red curve) are noticeably inconsistent with those obtained by directly solving the GKSL equation ρ_{NHTS}^S (red triangles) for the NH case in Fig. 7(a). In particular, $n_x > 1$ derived by ρ^I indicates that the results from choice I ρ^I are absurd and unphysical. Finally, we conclude that ρ^I is not a correct formulation for describing NH systems at finite- T .

Additionally, we have

$$\begin{aligned} \rho^I &= \hat{S}(e^{-\beta_T \hat{H}_0})\hat{S}^{-1} \\ &= e^{-\beta_T \hat{S} \hat{H}_0 \hat{S}^{-1}} = e^{-\beta_T \hat{H}_{\text{NH}}} \\ &= \rho^{\text{BZ}}. \end{aligned} \quad (\text{C5})$$

This equation means that n_i from $\rho^I = \hat{S}\rho_0\hat{S}^{-1}$ is the same as that from BZ distribution law $\rho^{\text{BZ}} = e^{-\beta_T \hat{H}_{\text{NH}}}$. The statement is also verified by Fig. 1(b) in the main text.

2. Choice II

In choice II, the expected values of physical operators σ_i ($i = x, y, z$) of the thermal \mathcal{PT} system are written as

$$n_i = \langle \sigma_i \rangle = \frac{1}{Z^{II}} \text{Tr}(\sigma_i \cdot \rho^{II}), \quad (\text{C6})$$

where $Z^{II} = \text{Tr}(\rho^{II})$ is the partition function.

After straightforward calculations, we have

$$\rho^{II} = \sigma_x A + \sigma_y B + \hat{I} C, \quad (\text{C7})$$

for the thermal \mathcal{PT} system, where $\hat{I} = \begin{pmatrix} 1 & 0 \\ 0 & 1 \end{pmatrix}$,

$$\begin{aligned} A &= -\sinh(\beta_T \sqrt{h^2 - \gamma^2}), \\ B &= \sinh(\beta_{\text{NH}}) \cdot \cosh(\beta_T \sqrt{h^2 - \gamma^2}), \\ C &= \cosh(\beta_{\text{NH}}) \cdot \cosh(\beta_T \sqrt{h^2 - \gamma^2}). \end{aligned} \quad (\text{C8})$$

Then, we get

$$\begin{aligned} n_x &= \frac{A}{C} = \frac{-\tanh(\beta_T \sqrt{h^2 - \gamma^2})}{\cosh \beta_{\text{NH}}}, \\ n_y &= 0, \\ n_z &= \frac{B}{C} = \tanh \beta_{\text{NH}}. \end{aligned} \quad (\text{C9})$$

The expected value of σ_i becomes real, i.e., $n_i = (n_i)^*$.

According to Fig. 7(b), the results from density matrix ρ^{II} (the red curve) are the same as those obtained by directly solving the GKSL equation ρ_{NHTS}^S (red triangles) for the NH case of $\gamma = 0.9$. In particular, $|n_x| \leq 1$ derived by ρ^{II} indicates that the results from choice II ρ^{II} are physical. This means that $\rho^{II} = \hat{S}\rho_0\hat{S}^\dagger$ is correct for the thermal \mathcal{PT} system in the NHTS.

-
- [1] C. M. Bender and S. Boettcher, *Phys. Rev. Lett.* **80**, 5243 (1998).
- [2] C. M. Bender, D. C. Brody, and H. F. Jones, *Phys. Rev. Lett.* **89**, 270401 (2002).
- [3] C. M. Bender, *Rep. Prog. Phys.* **70**, 947 (2007).
- [4] G. L. Giorgi, *Phys. Rev. B* **82**, 052404 (2010).
- [5] L. Ge and H. E. Türeci, *Phys. Rev. A* **88**, 053810 (2013).
- [6] C. Hang, G. Huang, and V. V. Konotop, *Phys. Rev. Lett.* **110**, 083604 (2013).
- [7] C. Korff and R. Weston, *J. Phys. A: Math. Theor.* **40**, 8845 (2007).
- [8] C. Korff, *J. Phys. A: Math. Theor.* **41**, 295206 (2008).
- [9] C. E. Rüter, K. G. Makris, R. El-Ganainy, D. N. Christodoulides, M. Segev, and D. Kip, *Nat. Phys.* **6**, 192 (2010).
- [10] A. Guo, G. J. Salamo, D. Duchesne, R. Morandotti, M. Volatier-Ravat, V. Aimez, G. A. Siviloglou, and D. N. Christodoulides, *Phys. Rev. Lett.* **103**, 093902 (2009).
- [11] P. Peng, W. Cao, C. Shen, W. Qu, J. Wen, L. Jiang, and Y. Xiao, *Nat. Phys.* **12**, 1139 (2016).
- [12] Z. Zhang, Y. Zhang, J. Sheng, L. Yang, M.-A. Miri, D. N. Christodoulides, B. He, Y. Zhang, and M. Xiao, *Phys. Rev. Lett.* **117**, 123601 (2016).
- [13] Y. D. Chong, L. Ge, and A. D. Stone, *Phys. Rev. Lett.* **106**, 093902 (2011).
- [14] A. Regensburger, C. Bersch, M.-A. Miri, G. Onishchukov, D. N. Christodoulides, and U. Peschel, *Nature (London)* **488**, 167 (2012).
- [15] L. Feng, Y.-L. Xu, W. S. Fegadolli, M.-H. Lu, J. E. B. Oliveira, V. R. Almeida, Y.-F. Chen, and A. Scherer, *Nat. Mater.* **12**, 108 (2013).
- [16] M. Wimmer, M.-A. Miri, D. Christodoulides, and U. Peschel, *Sci. Rep.* **5**, 17760 (2015).

- [17] S. Weimann, M. Kremer, Y. Plotnik, Y. Lumer, S. Nolte, K. G. Makris, M. Segev, M. C. Rechtsman, and A. Szameit, *Nat. Mater.* **16**, 433 (2017).
- [18] H. Hodaei, A. U. Hassan, S. Wittek, H. Garcia-Gracia, R. El-Ganainy, D. N. Christodoulides, and M. Khajavikhan, *Nature (London)* **548**, 187 (2017).
- [19] S. K. Özdemir, S. Rotter, F. Nori, and L. Yang, *Nat. Mater.* **18**, 783 (2019).
- [20] J. Li, A. K. Harter, J. Liu, L. de Melo, Y. N. Joglekar, and L. Luo, *Nat. Commun.* **10**, 855 (2019).
- [21] N. Bender, S. Factor, J. D. Bodyfelt, H. Ramezani, D. N. Christodoulides, F. M. Ellis, and T. Kottos, *Phys. Rev. Lett.* **110**, 234101 (2013).
- [22] J. Schindler, A. Li, M. C. Zheng, F. M. Ellis, and T. Kottos, *Phys. Rev. A* **84**, 040101(R) (2011).
- [23] S. Assaworarith, X. Yu, and S. Fan, *Nature (London)* **546**, 387 (2017).
- [24] Y. Choi, C. Hahn, J. W. Yoon, and S. H. Song, *Nat. Commun.* **9**, 2182 (2018).
- [25] S. Bittner, B. Dietz, U. Günther, H. L. Harney, M. Miski-Oglu, A. Richter, and F. Schäfer, *Phys. Rev. Lett.* **108**, 024101 (2012).
- [26] B. Peng, S. K. Özdemir, F. Lei, F. Monifi, M. Gianfreda, G. L. Long, S. Fan, F. Nori, C. M. Bender, and L. Yang, *Nat. Phys.* **10**, 394 (2014).
- [27] C. Poli, M. Bellec, U. Kuhl, F. Mortessagne, and H. Schomerus, *Nat. Commun.* **6**, 6710 (2015).
- [28] Z.-P. Liu, J. Zhang, S. K. Özdemir, B. Peng, H. Jing, X.-Y. Lü, C.-W. Li, L. Yang, F. Nori, and Y.-X. Liu, *Phys. Rev. Lett.* **117**, 110802 (2016).
- [29] L. Feng, Z. J. Wong, R. M. Ma, Y. Wang, and X. Zhang, *Science* **346**, 972 (2014).
- [30] H. Hodaei, M.-A. Miri, M. Heinrich, D. N. Christodoulides, and M. Khajavikhan, *Science* **346**, 975 (2014).
- [31] X. Zhu, H. Ramezani, C. Shi, J. Zhu, and X. Zhang, *Phys. Rev. X* **4**, 031042 (2014).
- [32] B.-I. Popa and S. A. Cummer, *Nat. Commun.* **5**, 3398 (2014).
- [33] R. Fleury, D. Sounas, and A. Alù, *Nat. Commun.* **6**, 5905 (2015).
- [34] K. Ding, G. Ma, M. Xiao, Z. Q. Zhang, and C. T. Chan, *Phys. Rev. X* **6**, 021007 (2016).
- [35] Y. Wu, W. Liu, J. Geng, X. Song, X. Ye, C. K. Duan, X. Rong, and J. Du, *Science* **364**, 878 (2019).
- [36] L. Herviou, N. Regnault, and J. H. Bardarson, *SciPost Phys.* **7**, 069 (2019).
- [37] P.-Y. Chang, J.-S. You, X. Wen, and S. Ryu, *Phys. Rev. Res.* **2**, 033069 (2020).
- [38] D. W. Zhang, Y. L. Chen, G. Q. Zhang, L. J. Lang, Z. Li, and S. L. Zhu, *Phys. Rev. B* **101**, 235150 (2020).
- [39] L.-M. Chen, Y. Zhou, S. A. Chen, and P. Ye, *Phys. Rev. B* **105**, L121115 (2022).
- [40] Z. Gong, Y. Ashida, K. Kawabata, K. Takasan, S. Higashikawa, and M. Ueda, *Phys. Rev. X* **8**, 031079 (2018).
- [41] G. Lindblad, *Commun. Math. Phys.* **48**, 119 (1976).
- [42] V. Gorini, A. Kossakowski, and E. C. G. Sudarshan, *J. Math. Phys.* **17**, 821 (1976).
- [43] H. P. Breuer and F. Petruccione, *The Theory of Open Quantum Systems* (Oxford University Press, Oxford, 2002).
- [44] Y. Aharonov, D. Z. Albert, and L. Vaidman, *Phys. Rev. Lett.* **60**, 1351 (1988); Y. Aharonov and L. Vaidman, *ibid.* **62**, 2327 (1989); A. J. Leggett, *ibid.* **62**, 2325 (1989); A. Peres, *ibid.* **62**, 2326 (1989); Y. Aharonov and L. Vaidman, *Phys. Rev. A* **41**, 11 (1990).
- [45] N. Matsumoto, K. Kawabata, Y. Ashida, S. Furukawa, and M. Ueda, *Phys. Rev. Lett.* **125**, 260601 (2020).
- [46] Y. Ashida and M. Ueda, *Phys. Rev. Lett.* **120**, 185301 (2018).
- [47] T. A. Brun, *Am. J. Phys.* **70**, 719 (2002).
- [48] B. Gardas, S. Deffner, and A. Saxena, *Sci. Rep.* **6**, 23408 (2016).
- [49] P. N. Meisinger and M. C. Ogilvie, *Philos. Trans. R. Soc. A* **371**, 20120058 (2013).
- [50] In choice I $\rho^1 = \sum_{n=\pm} |\Psi_n^R\rangle e^{-\beta_T E_n} \langle \Psi_n^L| = \hat{S}(e^{-\beta_T \hat{H}_0}) \hat{S}^{-1}$, the expected values of spin operator σ_i ($i = x, y, z$) are $n_x = -\cosh \beta_{\text{NH}} \cdot \tanh(\beta_T \sqrt{\hbar^2 - \gamma^2})$, $n_y = -i \sinh \beta_{\text{NH}} \cdot \tanh(\beta_T \sqrt{\hbar^2 - \gamma^2})$, $n_z = 0$. We find that the expected value of σ_y becomes imaginary, i.e., $n_y \neq (n_y)^*$ and the result is unphysical. See the detailed calculations in Appendix C.
- [51] R. Haag, N. Hugenholtz, and M. Winnink, *Commun. Math. Phys.* **5**, 215 (1967).